Monthly Notices
of the
ROYAL ASTRONOMICAL SOCIETY

MNRAS **476,** L50–L54 (2018)
Advance Access publication 2018 March 14

doi:10.1093/mnrasl/sly040

A system of three transiting super-Earths in a cool dwarf star

E. Díez Alonso,[1] S. L. Suárez Gómez,[1★] J. I. González Hernández,[2,3] A. Suárez Mascareño,[4] C. González Gutiérrez,[1] S. Velasco,[2,3] B. Toledo-Padrón,[2,3] F. J. de Cos Juez,[1★] and R. Rebolo[2,3,5]

[1]*Department of Exploitation and Exploration of Mines, University of Oviedo, E-33004 Oviedo, Spain*
[2]*Instituto de Astrofísica de Canarias, E-38205 La Laguna, Tenerife, Spain*
[3]*Dpto. Astrofísica, Universidad de La Laguna, E-38206 La Laguna, Tenerife, Spain*
[4]*Observatoire Astronomique de l' Université de Gèneve, CH-1290 Versoix, Switzerland*
[5]*Consejo Superior de Investigaciones Científicas, E-28006 Madrid, Spain*

Accepted 2018 March 12. Received 2018 March 9; in original form 2017 December 18

ABSTRACT

We present the detection of three super-Earths transiting the cool star LP415-17, monitored by K2 mission in its 13th campaign. High-resolution spectra obtained with High Accuracy Radial velocity Planet Searcher-North/Telescopio Nazionale Galileo (HARPS-N/TNG) showed that the star is a mid-late K dwarf. Using spectral synthesis models, we infer its effective temperature, surface gravity, and metallicity, and subsequently determined from evolutionary models a stellar radius of 0.58 $R_\odot$. The planets have radii of 1.8, 2.6, and 1.9 $R_\oplus$ and orbital periods of 6.34, 13.85, and 40.72 d. High-resolution images discard any significant contamination by an intervening star in the line of sight. The orbit of the furthest planet has radius of 0.18 au, close to the inner edge of the habitable zone. The system is suitable to improve our understanding of formation and dynamical evolution of super-Earth systems in the rocky–gaseous threshold, their atmospheres, internal structure, composition, and interactions with host stars.

Key words: techniques: photometric – techniques: spectroscopic – planets and satellites: detection – stars: individual: LP415-17 – stars: low mass

1 INTRODUCTION

Transiting planetary systems are of great value for the characterization of exoplanetary atmospheres (Charbonneau, Brown & Latham 2000; Kreidberg et al. 2014), the understanding of planetary formation and evolution (Owen et al. 1999), and for the study of the interactions with their host stars (Cauley et al. 2017). Cool dwarf stars are well suited to find Earth size and super-Earth size planets by the transit method, since transits produce deeper dimmings than in solar-type stars. The amplitude of signals in transit transmission spectroscopy is also higher for stars with small radius, favouring these type of stars for future atmospheric studies of their planetary systems (Gillon et al. 2016).

The Kepler mission (Borucki et al. 2010) has achieved a large number of detections of transiting planets (Howard et al. 2012). In its second mission (Howell et al. 2014), the satellite performs observations of different ecliptic plane fields for periods of time spanning about 80 d. Multiple signals of exoplanet candidates are present in concluded campaigns (Vanderburg et al. 2015; Crossfield et al. 2016). Campaign 13th has focused in the Hyades and Taurus region, centred in α = 04:51:11, δ = +20:47:11, between 2017 March 08 and 2017 May 27. In this campaign K2 observed 26.242 targets at standard long cadence mode and 118 targets at short cadence mode. LP415-17 (α = 04:21:52.487, δ = +21:21:12.96) has been observed in low cadence mode.

In this letter, we present the detection of three super-Earths transiting the star LP415-17 (EPIC 210897587, 2MASS 04215245 + 2121131). In Section 2 we describe the characterization of the star from spectra acquired with HARPS-N spectrograph and the analysis of the K2 photometric time series. We also discuss possible contaminating sources and the main parameters derived for the planets. In Section 3 we present estimations of the masses, discuss the stability of the system and its suitability for future characterization by transmission spectroscopy. In Section 4 we summarize the main conclusions derived from this work.

2 METHODS

2.1 Stellar characterization

We obtained three spectra, 1800 s of exposure time each, with HARPS-N (Cosentino et al. 2012) a fibrefed high-resolution echelle spectrograph installed at the 3.6 m Telescopio Nazionale Galileo in the Roque de los Muchachos Observatory (Spain) with a resolving

★ E-mails: fjcos@uniovi.es (FdC); suarezsergio@uniovi.es (SS)

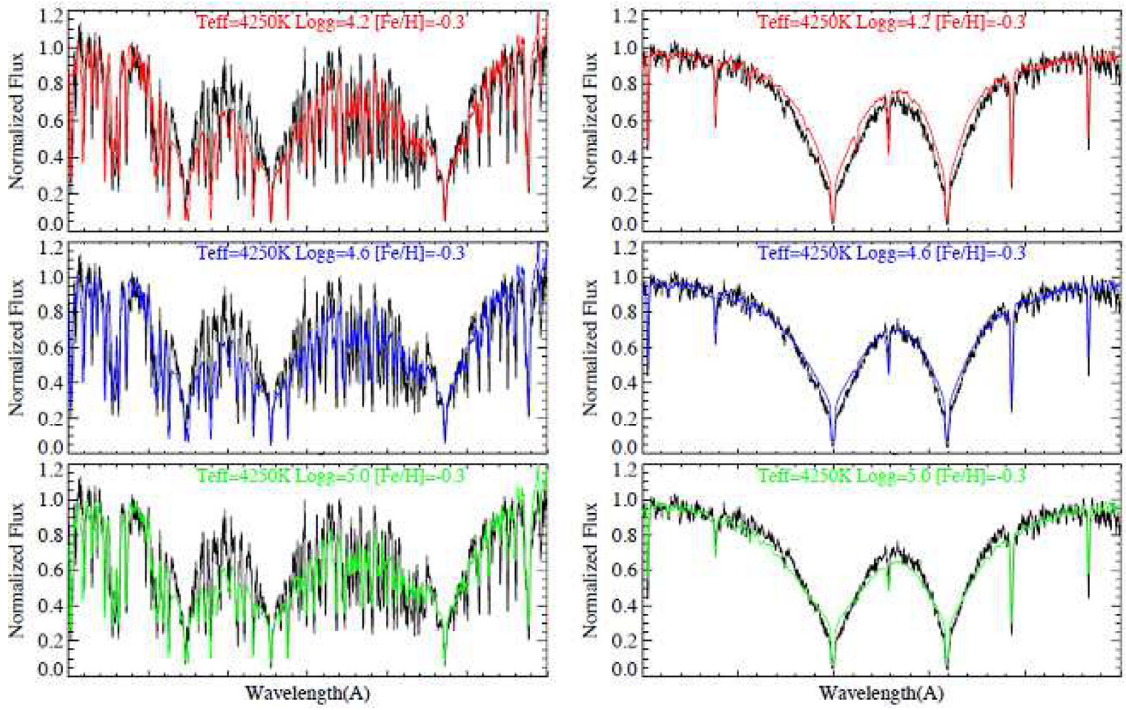

Figure 1. Synthetic spectral models centred in the magnesium triplet (left) and Na D doublet (right), calculated with $T_{\rm eff} = 4250$ K, [Fe/H]$= -0.3$, and $\log g = 3.4$ (top), $\log g = 4.6$ (middle), and $\log g = 4.0$ (bottom), compared with the observed spectrum. The best fit is obtained with $\log g = 4.6$.

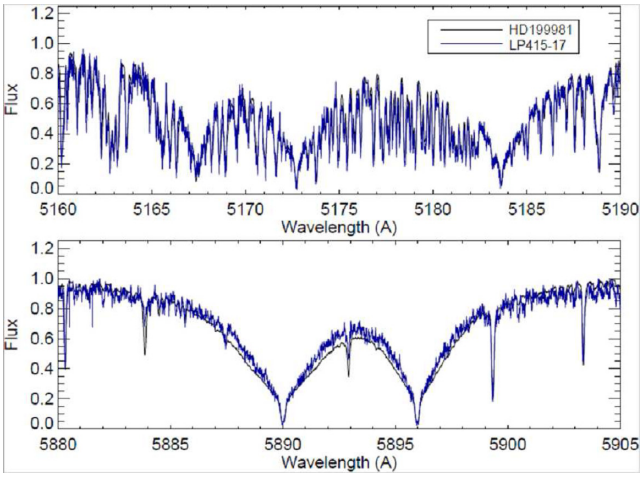

Figure 2. Spectrum of LP415-17 compared with the observed spectrum of HD199981.

power of $R = 115\,000$ over a spectral range from 380 to 690 nm. We have averaged them to obtain a final spectrum smoothed with 10-pixel step to improve the visualization of spectral features. We compared this spectrum with synthetic models (Allende Prieto et al. 2014) generated with ASSET (Koesterke et al. 2008), adopting Kurucz atmospheric models (Castelli & Kurucz 2003; Mészáros et al. 2012). Synthetic spectra have been broadened with a macroturbulence profile of 1.64 km s^{-1} (Fischer & Valenti 2005), with a rotation profile taking $v_{\rm rot} = 1.8$ km s^{-1} (Gray 2005) and with a Gaussian profile for instrumental broadening at resolution of 115 000 (FWHM $\sim$2.6 km s^{-1}). The effective temperature has been estimated using the infrared flux method (González Hernández & Bonifacio 2009). We apply $T_{\rm IRFM}$ – (colour, [Fe/H]) calibrations for dwarf stars, correcting for extinction the stellar magnitudes according to $A_X = R_X \times E(B-V)$. R_X was obtained from McCall (2004), and the reddening $E(B-V)$ from the dust maps (Schlegel et al. 1998), but corrected using the equations in Bonifacio et al. (2000) for the estimated distance to the star (82 pc) and Galactic latitude. We obtained $E(B-V) = 0.087$ and $T_{\rm IRFM} = 4258 \pm 150$ K.

The metallicity and $\log g$ have been obtained via comparison of the observed spectrum with synthetic spectra, resulting [Fe/H] $= -0.3 \pm 0.2$ and $\log g = 4.6 \pm 0.3$ (Fig. 1). We compare the stellar parameters and metallicity with a grid of tabulated isochrones (Bertelli et al. 1994), and obtain $R_* = 0.58^{+0.06}_{-0.03}$ R$_\odot$, $M_* = 0.65^{+0.06}_{-0.03}$ M$_\odot$, and $M_{\rm V} = 7.95^{+0.34}_{-0.66}$ mag. In Fig. 2 we compare the observed spectrum of LP415-17 with that of the well-characterized star HD199981 (Kordopatis et al. 2013), whose parameters (K6V, $T_{\rm eff} = 4263$ K, $\log g = 4.97$) are very close to our results for LP415-17.

Adopting $m_{\rm V} = 12.54$, we estimate a distance to LP415-17 of $D_* = 82^{+29}_{-12}$ pc. We measured a radial velocity from the HARPS-N spectrum, which combined with the proper motions reported in Table 1 results in velocity components $U = -38.2$ km s^{-1}, $V = -69.4$ km s^{-1}, and $W = 31.8$ km s^{-1}. A comparison with the kinematic and metallicity properties of the Copenhagen Survey of the Solar neighbourhood (Nordström et al. 2004) suggests that LP415-17 could be a member of the Hercules stream, which according to Bensby, Oey & Feltzing (2007) could be a combination of thin and thick disc stars originating in interactions of the inner disc with the bar of our Galaxy.

From the observed spectrum we determine a R'_{HK} index of -4.85 ± 0.13 which according to Suárez Mascareño et al. (2015) indicates a likely rotation period of 34.8 ± 8.2 d. Table 1 summarizes stellar parameters for LP415-17.

Table 1. Stellar parameters for LP415-17.

Parameter	Value	Source
V (mag)	12.806 ± 0.005	*a*
R (mag)	12.286 ± 0.006	*a*
I (mag)	12.289 ± 0.090	*a*
J (mag)	10.274 ± 0.021	*b*
H (mag)	9.686 ± 0.021	*b*
K (mag)	9.496 ± 0.014	*b*
$T_{\rm eff}$ (K)	4258 ± 150	*c*
[Fe/H]	-0.3 ± 0.2	*c*
Radius, $R_\odot$	$0.58^{+0.06}_{-0.03}$	*c*
Mass, $M_\odot$	$0.65^{+0.06}_{-0.03}$	*c*
$\log g$ (cgs)	4.6 ± 0.3	*c*
M_V (mag)	$7.95^{+0.34}_{-0.66}$	*c*
$\log_{10}(R'_{HK})$	-4.85 ± 0.13	*c*
$P_{\rm rot}$ (d)	34.8 ± 8.2	*c*
Distance (pc)	82^{+29}_{-12}	*c*
$V_{\rm r}$ (km s^{-1})	19.1 ± 0.5	*c*
μ_α (mas yr^{-1})	201.9 ± 6.9	*a*
μ_δ (mas yr^{-1})	-71.3 ± 4.3	*a*
U, V, W (km s^{-1})	$-38.2, -69.4, 31.8$	*c*

[a]UCAC4 (Zacharias et al. 2013).
[b]2MASS (Cutri et al. 2003).
[c]This work.

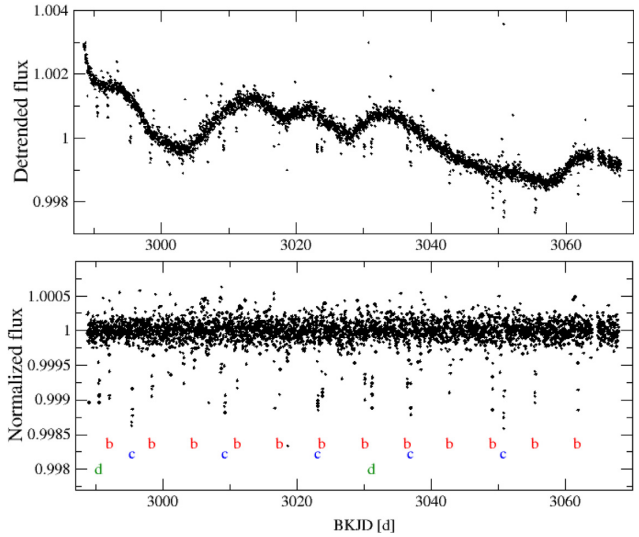

Figure 3. Top: K2 detrended light curve for LP415-17. Bottom: normalized light curve. Characters b, c, and d indicate times of observed transits of planets b, c, and d.

2.2 K2 photometric data

The light curve of LP415-17 exhibits clear signals of at least three transiting objects (Fig. 3). We analysed the K2 corrected photometry from the star following the work of Vanderburg & Johnson (2014), applying a spline fit to detrend stellar variability and search for periodic signals with a box least squares (BLS) method (Kovács et al. 2002) on flattened data. Once BLS finds a transit signal, it is fitted and removed, and another search for transit signals is performed. Following this method, we find three transit signals of planet candidates with orbital periods 6.342 ± 0.002 d (b), 13.850 ± 0.006 d (c), and 40.718 ± 0.005 d (d).

To estimate the main parameters for each planet we analysed each phase-folded transit using MCMC, fitting models from Mandel & Agol (2002) with the EXOFAST package (Eastman et al. 2013), resampling the light curve 10 times uniformly spaced over 29.4 min for each data point and averaging (Kipping 2010) (Fig. 4). We set priors on host star ($T_{\rm eff} = 4258$ K, $\log g = 4.6$, [Fe/H] $= -0.3$), orbital periods ($P_{\rm orb} = 6.34$ (b), 13.85 (c), 40.72 (d)) d. Due to tidal circularization, $e = 0$ for planet b. We also assume $e = 0$ for c and d, for being transiting planets in multiplanetary systems (Van Eylen & Albrecht 2015). The parameters obtained for planets b, c, and d are summarized in Table 2.

Planet d only shows two transits in the K2 13th campaign observation window. Separate analysis of these two transits reveals coincident transit parameters, supporting the idea that this signal is created by the same object. The parameters for each observed transit of planet d are summarized in Table 2.

The planets have estimated radii $1.8^{+0.2}_{-0.1}$ $R_\oplus$ (b), $2.6^{+0.7}_{-0.2}$ $R_\oplus$ (c), and $1.9^{+0.7}_{-0.2}$ $R_\oplus$ (d), orbital periods 6.342 ± 0.002 d (b), 13.850 ± 0.006 d (c), and 40.718 ± 0.005 d (d), and semimajor axis $0.0562^{+0.0013}_{-0.0014}$ au (b), $0.0946^{+0.0031}_{-0.0030}$ au (c), and $0.1937^{+0.0064}_{-0.0059}$ au (d).

2.3 False positives analysis

To exclude false positives from possible companions, we analysed speckle images of the star at 562 and 832 nm, obtained with NESSI at the 3.5 m WIYN telescope (Kitt peak, Arizona), available at ExoFOP-K2.[1,2] Images exclude companions at 0.2 arcsec with $\delta_{\rm mag} < 3.5$ and at 1 arcsec with $\delta_{\rm mag} < 6$. We searched for possible contaminating background sources in images from POSS-I (Minkowski & Abell 1963) (year 1953) and 2MASS (Cutri et al. 2003) (year 1998). LP415-17 exhibits high proper motion $\mu_\alpha = 201.9$ mas yr^{-1} and $\mu_\delta = -71.3$ mas yr^{-1} so we can inspect for background sources at LP415-17's position during the K2 13th campaign. No background object is found at the current star position (Fig. 5).

Speckle images from WIYN, inspection of POSS-I and 2MASS images, statistical analysis performed with VESPA package (Morton 2012, 2015) (obtaining FPP $< 10^{-5}$ for all the planets), and taking into account FPP overestimation for multiplanet systems (Lissauer et al. 2011; Sinukoff et al. 2016), make us to reject possible contaminating sources, concluding that the transit signals in LP 415-17 are of planetary origin.

3 DISCUSSION

Following the mass–radius relation (Weiss & Marcy 2014)

$$\frac{M_{\rm p}}{M_\oplus} = 2.69 \cdot \left(\frac{R_{\rm p}}{R_\oplus}\right)^{0.93}$$

for planets satisfying $1.5 \leq R_{\rm p}/R_\oplus \leq 4$, we obtain $M_{\rm b} = 4.7$ $M_\oplus$, $M_{\rm c} = 6.5$ $M_\oplus$, $M_{\rm d} = 4.9$ $M_\oplus$ for planets b, c, and d, respectively. Assuming $M_{\rm p} \ll M_*$, circular orbits, and $\sin i \sim 1$, we compute induced amplitudes in stellar velocity variations of 2.2 m s^{-1} for planet b, 2.3 m s^{-1} for planet c, and 1.2 m s^{-1} for planet d.

Given the visual magnitude of the star ($V = 12.8$) the required radial velocity monitoring at 1 m s^{-1} precision is hard to obtain for HARPS-like spectrographs in medium size telescopes, however is well suited for ESPRESSO (Pepe et al. 2014; González Hernández,

[1]https://exofop.ipac.caltech.edu/k2/
[2]Images where taken by Hirano et al. (2018). We noticed their work in this system during the revision process.

Table 2. Parameters for planets b, c, and d.

Planet parameters	*b*	*c*	*d*		
Orbital period, P (d)	6.342 ± 0.002	13.850 ± 0.006	40.718 ± 0.005		
Semimajor axis, a (au)	$0.0562^{+0.0013}_{-0.0014}$	$0.0946^{+0.0031}_{-0.0030}$	$0.1937^{+0.0064}_{-0.0059}$		
Radius, R_p ($R_\oplus$)	$1.8^{+0.2}_{-0.1}$	$2.6^{+0.7}_{-0.2}$	$1.9^{+0.7}_{-0.2}$		
Mass, M_p ($M_\oplus$)[a]	$4.7^{+0.5}_{-0.3}$	$6.5^{+1.5}_{-0.5}$	$4.9^{+1.7}_{-0.6}$		
Equilibrium temperature, T_{eq} (K)	708^{+38}_{-31}	583^{+52}_{-35}	381^{+47}_{-25}		
Transit parameters	*b*	*c*	*d*	*d* (2990.500)[b]	*d* (3031.218)[b]
Number of transits	12	5	2	–	–
Epoch, BKJD (d)	2992.068 ± 0.002	2995.426 ± 0.001	2990.500 ± 0.003	2990.500 ± 0.003	3031.218 ± 0.002
Radius of planet in stellar radii (R_p/R_*)	$0.0261^{+0.0009}_{-0.0008}$	$0.0321^{+0.0016}_{-0.0010}$	$0.0273^{+0.0021}_{-0.0015}$	$0.0280^{+0.0011}_{-0.0009}$	$0.0292^{+0.0027}_{-0.0018}$
Semimajor axis in stellar radii (a/R_*)	$18.5.0^{+1.1}_{-1.6}$	$27.0^{+2.2}_{-4.2}$	$63.3^{+6.4}_{-13}$	$73.2^{+4.2}_{-6.7}$	75.0^{+13}_{-20}
Linear limb-darkening coeff, u_1	$0.644^{+0.063}_{-0.080}$	$0.614^{+0.065}_{-0.084}$	$0.597^{+0.085}_{-0.110}$	$0.551^{+0.083}_{-0.11}$	$0.540^{+0.10}_{-0.12}$
Quadratic limb-darkening coeff, u_2	$0.122^{+0.074}_{-0.061}$	$0.148^{+0.071}_{-0.060}$	$0.142^{+0.091}_{-0.072}$	$0.174^{+0.093}_{-0.077}$	$0.183^{+0.11}_{-0.088}$
Inclination, i (deg)	$88.3^{+1.2}_{-1.9}$	$88.96^{+0.71}_{-0.88}$	$89.61^{+0.27}_{-0.48}$	$89.75^{+0.17}_{-0.20}$	$89.62^{+0.26}_{-0.37}$
Impact parameter, b	$0.34^{+0.24}_{-0.23}$	$0.45^{+0.37}_{-0.31}$	$0.44^{+0.33}_{-0.30}$	$0.33^{+0.20}_{-0.21}$	$0.50^{+0.22}_{-0.31}$
Transit depth, δ	$0.00068^{+0.00005}_{-0.00004}$	$0.00103^{+0.00010}_{-0.00006}$	$0.00074^{+0.00012}_{-0.00008}$	$0.00078^{+0.00006}_{-0.00005}$	$0.00085^{+0.00017}_{-0.00010}$
Total duration, T_{14} (d)	$0.1004^{+0.0050}_{-0.0048}$	$0.1470^{+0.0130}_{-0.0260}$	$0.1860^{+0.0097}_{-0.0018}$	$0.1713^{+0.0056}_{-0.0051}$	$0.156^{+0.018}_{-0.011}$
Ingress/egress duration, τ (d)	$0.0030^{+0.0009}_{-0.0003}$	$0.0056^{+0.0039}_{-0.0008}$	$0.0060^{+0.0050}_{-0.0010}$	$0.0052^{+0.0014}_{-0.0005}$	$0.0058^{+0.0049}_{-0.0016}$

[a]The masses are estimated using mass–radius relation from Weiss & Marcy (2014).
[b]Derived parameters for individual transits of planet d.

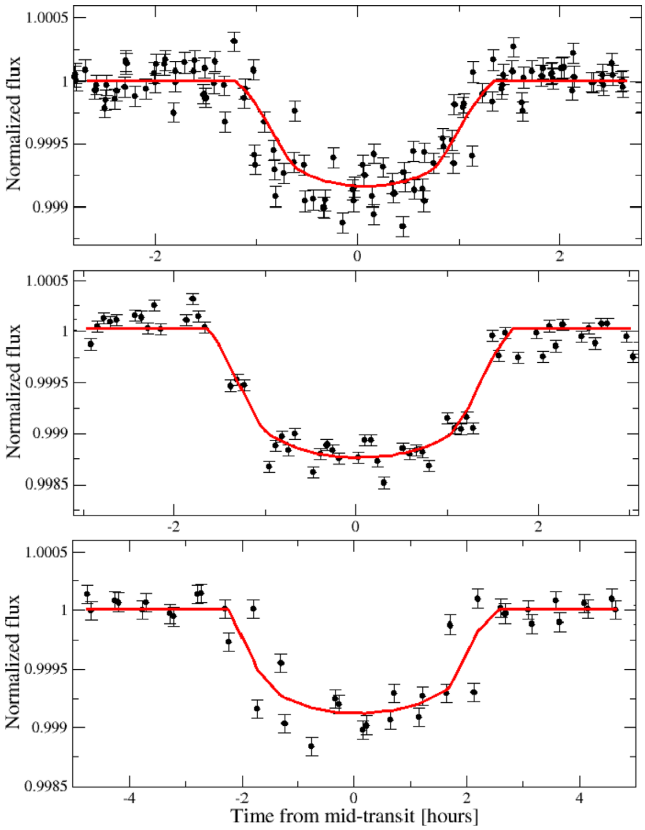

Figure 4. Phase-folded light curves corresponding to planets b (top), c (middle), and d (bottom). Solid curves represent best model fits obtained by MCMC.

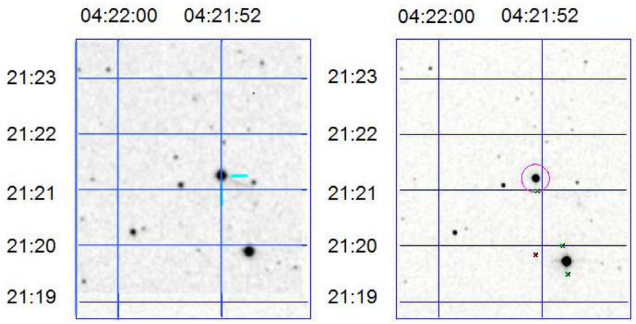

Figure 5. POSS-I image (1953, left) and 2MASS (1998, right). No background source is present at star's position in K2 13th campaign.

Pepe & Molaro 2017) at the Very Large Telescope (VLT). The moderated chromospheric activity of the star is likely to induce RV signals of order less than 3 m s^{-1} (Suárez Mascareño et al. 2017) which should not prevent the detection of the dynamical signals induced by the planets and the determination of their masses and densities. We estimate the incident flux for planet d as $F_p = 2.63$ $F_\oplus$. Habitable zone estimations (Kane et al. 2016) place the inner edge of the habitable zone at 1.5 $F_\oplus$, so planets b, c, and d are closer to the star than the inner part of the habitable zone.

The amplitude of the signal in transit transmission spectroscopy can be estimated as $\frac{R_p \cdot h_{eff}}{(R_*)^2}$ (Gillon et al. 2016) with h_{eff} the effective atmospheric height, which is related to the atmospheric scale height $H = K{\cdot}T/\mu{\cdot}g$ (K Boltzmann's constant, T atmospheric temperature, μ atmospheric mean molecular mass, g surface gravity). We adopt $h_{eff} = 7H$ (Miller-Ricci & Fortney 2010) for a transparent volatile dominated atmosphere ($\mu = 20$) with 0.3 Bond albedo. With these assumptions we estimate the amplitudes of transit trans-

mission spectroscopy signals as 2.2×10^{-5} (b), 3.5×10^{-5} (c), and 1.2×10^{-5} (d).

We tested the stability of the system simulating its evolution for 10^6 yr with the MERCURY package (Chambers 1999), using Bulirsch–Stoer integrator, adopting circular orbits and masses from the mass–radius relation. Our simulations show no significant changes in the eccentricity (always below 0.0005 for all the planets) or in the inclination of the orbits (always below 1.6°, 1.2°, and 1° for planets b, c, and d), pointing towards a dynamically stable system.

4 CONCLUSIONS

We presented a system with three transiting super-Earths orbiting a mid-late type K dwarf star, discovered with photometric data from K2. The star has been studied and characterized in detail, analysing its spectrum and long-time photometric series. The detected planets have radii $1.8^{+0.2}_{-0.1}$ $R_\oplus$ (b), $2.6^{+0.7}_{-0.2}$ $R_\oplus$ (c), and $1.9^{+0.7}_{-0.2}$ $R_\oplus$ (c), and orbital periods 6.342 ± 0.002 d (b), 13.850 ± 0.006 d (c), and 40.718 ± 0.005 d (d). Additional photometric monitoring is required to confirm planet d and radial velocity monitoring with ultrastable spectrographs at 8–10 m telescopes is necessary to determine accurate planetary masses. The amplitudes of atmospheric signals in transmission spectroscopy have been estimated at ∼20 ppm, making the system a good target to incoming facilities such as *James Webb Telescope*.

ACKNOWLEDGEMENTS

EDA, SLSG, CGG, and FJCJ acknowledge Spanish ministry projects MINECO AYA2014-57648-P and AYA2017-89121-P, and the regional grant FC-15-GRUPIN14-017. JIGH, BTP, and RRL acknowledge the Spanish ministry project MINECO AYA2014-56359-P. JIGH also acknowledges financial support from the Spanish Ministry of Economy and Competitiveness (MINECO) under the 2013 Ramón y Cajal program MINECO RYC-2013-14875. ASM acknowledges financial support from the Swiss National Science Foundation (SNSF).

REFERENCES

Allende Prieto C. et al., 2014, A&A, 568, A7
Bensby T., Oey M. S., Feltzing S., Gustafsson B., 2007, ApJ, 655, L89
Bertelli G., Bressan A., Chiosi C., Fagotto F., Nasi E., 1994, A&AS, 106, 275
Bonifacio P., Monai S., Beers T. C., 2000, AJ, 120, 2065
Borucki W. J. et al., 2010, Science, 327, 977
Castelli F., Kurucz R. L., 2003, in Piskunov N., Weiss W. W., Gray D. F. eds. Proc. IAU Symp. 210, Modelling of Stellar Atmospheres. Astron. Soc. Pac., San Francisco, p. A20
Cauley P. W., Redfield S., Jensen A. G., 2017, AJ, 153, 185
Chambers J. E., 1999, MNRAS, 304, 793
Charbonneau D., Brown T. M., Latham D. W., Mayor M., 2000, ApJ, 529, L45
Cosentino R., et al., 2012, in McLean I. S., Ramsay S. K., Takami H. eds. Proc. SPIE Conf. Ser. Vol. 8446, Ground-based and Airborne Instrumentation for Astronomy IV, SPIE, Bellingham, p. 84461V
Crossfield I. J. M. et al., 2016, ApJS, 226, 7
Cutri R. M. et al., 2003, VizieR Online Data Catalog, 2246
Eastman J., Gaudi B. S., Agol E., 2013, PASP, 125, 83
Fischer D. A., Valenti J., 2005, ApJ, 622, 1102
Gillon M. et al., 2016, Nature, 533, 221
González Hernández J. I., Bonifacio P., 2009, A&A, 497, 497
González Hernández J. I. Pepe F. Molaro P. Santos N. 2017, preprint (arXiv: 1711.05250)
Gray D. F. 2005, The Observation and Analysis of Stellar Photospheres. Cambridge Univ. Press, Cambridge
Hirano T. et al., 2018, preprint (arXiv:1801.06957)
Howard A. W. et al., 2012, ApJS, 201, 15
Howell S. B. et al., 2014, PASP, 126, 398
Kane S. R. et al., 2016, ApJ, 830, 1
Kipping D. M., 2010, MNRAS, 408, 1758
Koesterke L., Allende Prieto C., Lambert D. L., 2008, ApJ, 680, 764
Kordopatis G. et al., 2013, AJ, 146, 134
Kovács G., Zucker S., Mazeh T., 2002, A&A, 391, 369
Kreidberg L. et al., 2014, Nature, 505, 69
Lissauer J. J. et al., 2011, ApJS, 197, 8
Mandel K., Agol E., 2002, ApJ, 580, L171
McCall M. L., 2004, AJ, 128, 2144
Mészáros S. et al., 2012, AJ, 144, 120
Miller-Ricci E., Fortney J. J., 2010, ApJ, 716, L74
Minkowski R. L., Abell G. O., 1963, Basic Astronomical Data: Stars and Stellar Systems . University of Chicago Press, Chicago, USA, p. 481
Morton T. D., 2012, ApJ, 761, 6
Morton T. D. 2015, Astrophysics Source Code Library, record ascl:1503.011
Nordström B. et al., 2004, A&A, 418, 989
Owen T., Mahaffy P., Niemann H. B., Atreya S. Donahue T., Bar-Nun A., de Pater I., 1999, Nature, 402, 269
Pepe F. et al., 2014, Astron. Nachr., 335, 8
Schlegel D. J., Finkbeiner D. P., Davis M., 1998, ApJ, 500, 525
Sinukoff E. et al., 2016, ApJ, 827, 78
Suárez Mascareño A., Rebolo R., González Hernández J. I., Esposito M., 2015, MNRAS, 452, 2745
Suárez Mascareño A., Rebolo R., González Hernández J. I., Esposito M., 2017, MNRAS, 468, 4772
Van Eylen V., Albrecht S., 2015, ApJ, 808, 126
Vanderburg A., Johnson J. A., 2014, PASP, 126, 948
Vanderburg A. et al., 2015, ApJ, 800, 59
Weiss L. M., Marcy G. W., 2014, ApJ, 783, L6
Zacharias N., Finch C. T., Girard T. M., Henden A., Bartlett J. L., Monet D. G., Zacharias M. I., 2013, AJ, 145, 44

This paper has been typeset from a TEX/LATEX file prepared by the author.